Cell Calcium 45 (2009) 177–184

Contents lists available at ScienceDirect

Cell Calcium

journal homepage: www.elsevier.com/locate/ceca

Phosphatidylserine externalization in caveolae inhibits Ca^{2+} efflux through plasma membrane Ca^{2+}-ATPase in ECV304

Jie Zhang[a,c,1], Ping Xiao[b,1], Xujia Zhang[a,*]

[a] National Laboratory of Biomacromolecules, Institute of Biophysics, Chinese Academy of Sciences, 15 Datun Road, Chaoyang District, Beijing 100101, China
[b] College of Biology, Beijing Forestry University, Beijing 100083, China
[c] College of Pharmaceutical Sciences, Zhejiang University, Hangzhou, Zhejiang 310058, China

ARTICLE INFO

Article history:
Received 18 April 2008
Received in revised form 30 July 2008
Accepted 7 September 2008
Available online 16 October 2008

Keywords:
PMCA
Caveolae
ATPase
Ca^{2+}
Phosphatidylserine

ABSTRACT

It has been evidenced that plasma membrane Ca^{2+}-ATPase (PMCA) is localized at caveolae. However, the caveolar function of PMCA in living cells has never been demonstrated. In the present study, PMCA is exclusively localized at caveolae from ECV 304 cells demonstrated by sucrose gradient fractionation and the co-localization of PMCA with caveolin-1 was visualized by confocal microscopy. We found that PMCA is the main mechanism involved in Ca^{2+} efflux in ECV 304 cells. Treatment of cells with MβCD to disrupt caveolae significantly reduced the Ca^{2+} efflux, and the rate of decay is $4.45 \pm 0.14\ min^{-1}$ in the absence of MβCD and $1.99 \pm 0.038\ min^{-1}$ in the presence of MβCD. Moreover, the replenishment of cholesterol restored the reduction of the PMCA-mediated Ca^{2+} efflux in the presence of MβCD. Consistent with Ca^{2+} efflux in living cells, the activity of the reconstituted PMCA in membranes extracted from cells in vitro was decreased in the presence of MβCD. It was found that phosphatidylserine, which is normally in the inner leaflet of plasma membranes and is able to stimulate PMCA was relatively enriched in caveolae. Importantly, the treatment of cells with MβCD concomitantly increased the phosphatidylserine externalization. Taken together, our results suggest that activation of PMCA in caveolae is modulated by phosphatidylserine, and phosphatidylserine externalization induced by MβCD reduced the interaction of phosphatidylserine with PMCA, subsequently PMCA-mediated Ca^{2+} efflux in ECV 304 cells.

Published by Elsevier Ltd.

1. Introduction

Caveolae, a subclass of lipid rafts, are 60–80 nm diameter invaginations of the plasma membrane and contain the marker protein caveolin [1–4]. Caveolae are enriched with sphingolipids and cholesterol, and are resistant to detergent extraction relative to the other parts of the plasma membrane and other cellular membranes [5–7]. Caveolae are also enriched in phosphatidylserine (PS), an anionic aminophospholipid, which is mostly sequestered in the inner leaflet of the plasma membrane [8,9]. Many plasma membrane receptors and transporters are highly concentrated in caveolae, leading to speculation that this localization is important for their function. However, it is not well understood how this clustering contributes to their regulation and function [10–12].

The plasma membrane Ca^{2+}-ATPase (PMCA) is a P-type ATPase that plays a crucial role in regulation of cell calcium homeostasis [13,14]. It functions to pump Ca^{2+} from the cytosol to the extracellular space, maintaining a low resting intracellular calcium concentration. The pump shares the catalytic properties of ion-motive ATPases of the P-type family. It has 10 transmembrane segments (M1–M10) with most of its regulatory domains exposed to the cytosol. Its distinctive regulatory properties are conferred by its long (~150 amino acids) C-terminal intracellular tail [15], which contains a calmodulin-binding autoinhibitory domain. The binding of calmodulin enhances both the Ca^{2+} sensitivity and the turnover of the pump [16,17]. Additionally, PMCA can be activated by acidic lipids including PS [18]. This effect is mediated by two domains, one located near the C-terminus, the other a highly charged segment of about 60 amino acids between loops M2 and M3 [19–21].

It has been evidenced that PMCA is localized in caveolae [22,23]. It was recently shown that PMCA is localized and active in caveolae isolated from proximal kidney tubules, and the activity of PMCA is dependent upon the integrity of caveolae [24]. In contrast, the reconstituted PMCA in liposomes prepared with defined lipids indicates that the enzyme has higher activity in non-caveolae/lipid rafts portion [25]. So far, there is no data reporting the Ca^{2+} efflux from caveolar PMCA in living cells. In the present study, we studied the PMCA-mediated Ca^{2+} efflux in human umbilical vein endothelial

* Corresponding author. Tel.: +86 10 6488 8517; fax: +86 10 6487 2026.
E-mail address: xjzhang@sun5.ibp.ac.cn (X. Zhang).
[1] These authors contributed equally to this work.

0143-4160/$ – see front matter. Published by Elsevier Ltd.
doi:10.1016/j.ceca.2008.09.002

ECV304 cells. It was shown that PMCA is localized at caveolae, and the PMCA-mediated Ca^{2+} efflux was impaired after caveolae disruption by MβCD. In addition, externalization of PS was also modulated by cholesterol depletion, suggesting that PS could contribute to the activation of caveolar PMCA.

2. Materials and methods

2.1. Materials

ECV304 cell lines were kindly provided by Dr. Xiyun Yan (Institute of Biophysics, Chinese Academy of Sciences, China). Plasmid pCDNA3.0 containing caveolin-1 gene was a gift of Dr. Pingsheng Liu (Institute of Biophysics, China). Mouse anti-human PMCA IgG antibody (5F10), horseradish peroxidase (HRP)-conjugated secondary antibody and Protein A/G plus-Agarose were from Santa Cruz Biotechnology. Mouse anti-human caveolin-1 IgM antibody was from BD Biosciences. Annexin V-FITC kit was from JingMei Biotechnology. Cholesterol quantification kit was from Biosino Bio-technology and Science Inc. Fetal bovine serum, Lipofectamine™ 2000, OPTI-MEM Transfection Medium were all from Invitrogen. Phosphatidylcholine, sphingomyelin, cholesterol, *N*-methyl-D-glucamine, thapsigargin (TG), oligomycin, ionomycin, methyl-β-cyclodextrin (MβCD) were all from Sigma. Calmodulin–sephorose Cl-4B was from Pharmacia. Bio-beads were from Bio-Rad. All other reagents used were of analytical grade.

2.2. Methods

2.2.1. Purification of plasma membrane (Ca^{2+}–Mg^{2+})-ATPase from pig erythrocyte ghosts

Pig erythrocyte ghosts were prepared from fresh blood according to the procedure described by Haaker and Racker [26] with some modifications. Fresh pig blood (1 l, containing heparin sodium of 0.1–0.2 mg/ml blood) was centrifuged at 5800 × *g* for 10 min and washed four times in 130 mM KCl, 10 mM Tris-HCl (pH 7.4) (buffer I). Red cells were then lysed in 10× volumes of 1 mM EDTA, 10 mM Tris-HCl (pH 7.4) (buffer II). The hemolysate was then centrifuged at 20,000 × *g* for 35 min. The pellet was thoroughly washed several times with buffer II and 10 mM Hepes/KOH (pH 7.4) (buffer III). Discarded the very firm red pellet (blood blot) every step, and kept the milky pellet (ghosts) on the top of the red part. Finally, the ghosts was resuspended in 10 mM Hepes/KOH (pH 7.4), 130 mM KCl, 0.5 mM $MgCl_2$, 0.05 mM $CaCl_2$ (buffer IV), and stored at −80 °C until used.

Ghosts (6 mg/ml) in 10 mM Hepes/KOH (pH 7.4), 300 mM KCl, 1 mM $MgCl_2$, 100 μM $CaCl_2$, 0.1 mM PMSF, 10 mM 2-mercaptoethanol and 15% (w/v) glycerol was solubilized by the addition of Triton X-100 to a final concentration of 0.6% (w/v) and agitated slowly on ice for 15 min. After centrifugation at 125,000 × *g* for 30 min, the supernatant was applied onto a CaM-affinity column and washed roughly with a buffer containing 100 μM Ca^{2+}. PMCA was eluted from the column with a buffer containing 2 mM EDTA instead of any Ca^{2+} and Triton X-100 0.06% (w/v) other than 0.6% (w/v). After the chromatography column, fractions containing maximum protein concentration and ATPase activity were collected. Add $MgCl_2$ and $CaCl_2$ to the collection to a concentration of 1 and 0.1 mM, respectively. Aliquots of the purified PMCA was quickly frozen in liquid N_2, and stored at −80 °C. The protein concentration was determined by using the slight modification of the Lowry et al. procedure to avoid any interference by Triton X-100 and 2-mercaptoethanol, using bovine serum albumin as a standard.

2.2.2. Reconstitution of the purified ATPase by the Bio-beads

The reconstitution protocol was that described by Niggli et al. [18], except that 80 mg/ml Bio-beads were added to the mixture of designated lipids solution and ATPase every hour for three times and the mixture was agitated slowly at room temperature. In some cases, total cell lipids were extracted by chloroform/methanol method.

2.2.3. Cell culture, plasmids construction, and transfections

ECV304 cells were grown in RPMI-1640 medium supplemented with 10% fetal bovine serum, penicillin (50 unit/ml), and streptomycin (50 mg/ml), at 37 °C in an atmosphere of 5% CO_2/95% air. Caveolin-1 gene from pCDNA3.0 plasmid was cloned into pERFP-N1 plasmid (a mutant of pEGFP-N1) at the multiple cloning sites of EcoRI and XhoI. When ECV304 cells were 50–70% confluent, plasmid pEGFP–PMCA4b and pERFP–cav1 were co-transfected into cells using Lipofectamine™ 2000 according to the manufacturer's instructions. After 24–48 h, the cells were monitored for GFP-fusing protein expression using Olympus FV-500 Confocal Imaging System.

2.2.4. Cholesterol depletion and replenishment

Cholesterol depletion and replenishment were performed according to that described by Gingras et al. [27] with some modifications. For cholesterol removal, cell monolayers were washed with PBS and incubated for 30 min at 37 °C with buffer A (10 mM Hepes/KOH, pH 7.4, 5 mM KCl, 1 mM $MgCl_2$, 100 μM EGTA, 140 mM *N*-methyl-D-glucamine, 10 mM glucose) in the absence or presence of 10 mM MβCD. For cholesterol replenishment, cholesterol (0.25 mM, final concentration) was added to buffer A containing 2.5 mM MβCD and the mixture was incubated clear at 37 °C by discontinuous vortexing. To replenish cellular cholesterol, MβCD-treated cells were incubated in cholesterol/MβCD mixture at 37 °C for 1 h. After 1 h, the medium was removed and the cells were washed to remove the MβCD. Following either cholesterol depletion or replenishment, the cells were processed as required for each experiment.

2.2.5. Flow cytometric analysis of phosphatidylserine externalization

ECV304 cells were harvested by trypsinization, washed and resuspended in buffer A at 1 × 10^6 cells/ml. Then aliquots of 500-μl cells were treated by MβCD or followed by cholesterol replenishment (see above). Untreated cells were used as controls. Then all the aliquots were collected by centrifugation, washed and resuspended in 100 μl binding buffer (10 mM Hepes/KOH, pH 7.4, 140 mM NaCl, 2.5 mM $CaCl_2$) and labeled with 10 μl Annexin V-FITC probes for 10–20 min at room temperature. Additional 400 μl binding buffer was added to each aliquot and phophatidylserine externalization was analyzed by flow cytometry. Unlabeled cells were used as negative controls.

2.2.6. Isolation of caveolae-enriched membrane domains and Western blot analysis

Low-density caveolae-enriched membrane domains were prepared as described by Gingras et al. [27]. All the procedures were performed at 4 °C. Confluent ECV304 cells cultured on 75 cm^2 flasks (containing about 2 × 10^7 cells) were scraped into 0.6 ml of 0.5 M sodium carbonate (pH 11). At 30% of maximal power, the cells were sonicated for six times with each time 20 s (pulse on 5 s/off 5 s) at a 2-min interval. The resulting homogenate was made up to 45% sucrose by the addition of 0.6 ml 90% sucrose in Mes-buffered saline (MBS: 25 mM Mes, pH 6.5, 150 mM NaCl) and overlaid with two layers of 35% and 5% sucrose in MBS containing 0.25 M carbonate

(1.2 ml each). The gradient was then centrifuged at 200,000 × *g* for 20 h using a Beckman SW55Ti rotor.

For the analysis of the resulting gradient, 0.3-ml fractions were collected from the top of the gradient and 20 μl of the fractions were subjected to SDS-PAGE on 10% polyacrylamide gels and electroblotted onto PVDF membranes using standard procedures. Blots were blocked overnight at with 3% BSA in Tris-buffer saline (TBS: 10 mM Tris/HCl, pH 7.4, 150 mM NaCl) followed by a 1-h incubation with the primary antibody. Immunoreactive bands were visualized by a 1-h incubation with HRP-conjugated secondary antibodies followed by enhanced chemiluminescence (ECL) method.

2.2.7. PMCA activity assay in individual cells in vivo

ECV304 cells were plated onto 35 mm confocal chambers and grew overnight to about 50% confluence during the log phase of growth. After washing with PBS, the cells were labeled with 5 μM Fura-2/AM in serum-free RPMI1640 for 45 min at 37 °C. Then the cells were washed to remove extracellular probes and incubated in Ca^{2+}-free medium (10 mM Hepes/KOH, pH 7.4, 5 mM KCl, 1 mM $MgCl_2$, 100 μM EGTA, 140 mM *N*-methyl-D-glucamine, 10 mM glucose). The chambers were mounted on Olympus IX-71 Inverted Fluorescence Microscopy. Fluorescence was recorded with excitation wavelengths of 340 and 380 nm and emission at 520 nm. Changes in $[Ca^{2+}]_i$ were monitored using the Fura-2 340/380 fluorescence ratio (F340/F380). Thapsigargin was used to block ER Ca^{2+}-ATPase and deplete the intracellular calcium stores. To compare the rates of decay of $[Ca^{2+}]_i$ to basal values, Fura-2/AM labeled cells were either treated by MβCD (sometimes followed by cholesterol replenishment) or untreated (control) before calcium measurement.

All the data were processed and analyzed using the exponential decay arithmetic of the OriginPro7.5 program for $[Ca^{2+}]_i$ decay analysis.

2.2.8. DPH labeling and fluorescence measurement

The fluorescence probe of DPH was dispersed into proteoliposome suspension at a probe-to-lipid molar ratio of 1:500, then incubated at 37 °C for 1 h in the dark. Fluorescence polarization measurements were determined on a Hitachi F-4500 spectrofluorimeter fitted with a polarization attachment as described by Shinitzky and Barenholz [28]. The samples were excited at 360 nm, and the emissions at 430 nm were recorded. Both excitation and emission slits were set at 5 nm. The degree of fluorescence polarization (P), which reflects the motion and viscosity of lipid molecules, was calculated according to the following formula: $P = (I_{VV} - GI_{VH})/(I_{VV} + GI_{VH})$ [29], where I_{VV} and I_{VH} are the fluorescence intensities measured with parallel and perpendicular oriented polarizers, respectively, and G is the calibration factor. Here, $G = I_{HV}/I_{HH}$, V = 90, H = 0.

3. Results

3.1. Co-localization of PMCA and caveolin-1 in caveolae from ECV 304 cells

Caveolae were isolated from ECV 304 cells by a well-established density gradient fractionation procedure and the distribution of PMCA and caveolin-1 in each fraction was determined by Western blot (Fig. 1). Consistent with previous observations of caveolae fractionation by the same procedure, caveolin-1 was only found in the low density, cholesterol-rich fractions of the sucrose gradient (fractions 4–6). The PMCA distribution, detected by both the monoclonal antibody anti-PMCA (5F10) and the isoform-specific antibody anti-PMCA4b, was similar to that of caveolin-1 (Fig. 1a).

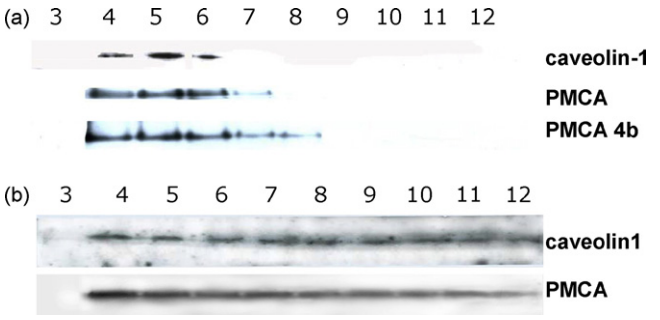

Fig. 1. Co-localization of PMCA and caveolin-1 in caveolae from EVC 304 cells. Samples of lysates (2×10^7 cells) were fractionated by the detergent-free carbonate-based procedure, and 12 fractions of equal volume (0.3 ml each) were collected (see Section 2). 20 μl of each fraction was subjected to SDS-PAGE, and Western blot analysis of PMCA and caveolin-1 with the indicated antibodies was performed in the absence (a) and presence (b) of MβCD.

This result was consistent with other reports that PMCA4b is localized in caveolae/lipid rafts.

MβCD selectively depletes cholesterol from plasma membranes, thereby disrupting caveolae whose integrity depends on cholesterol. After incubation of ECV 304 cells in 10 mM MβCD for 30 min, the cholesterol concentration in caveolae was dramatically reduced (data not shown). Accordingly, both caveolin-1 and PMCA spread along the entire gradient (Fig. 1b), indicating that caveolae had been disrupted.

As an additional test of the localization of PMCA, ECV 304 cells were co-transfected with caveolin-1–ERFP and PMCA4b–EGFP. Both caveolin-1 and PMCA were distributed on the plasma membrane. Significantly, Fig. 2 shows considerable overlap of caveolin-1 and PMCA, which is fully consistent with the biochemical results. We conclude that PMCA is localized to caveolae in ECV 304 cells.

3.2. PMCA-mediated Ca^{2+} efflux in ECV 304 cells

An understanding of the function of PMCA in living cells and tissues is hampered by the absence of specific pharmacological inhibitors of PMCA. PMCA-mediated Ca^{2+} efflux is currently measured in vivo by isolating its contribution from that of other calcium regulatory processes by selectively inhibiting the major alternative Ca^{2+} transporting pathways [30,31]. In the present study we inhibited the sarco/endoplasmic reticulum Ca^{2+}-ATPase (SERCA) using 5 μM TG (the specific inhibitor of SERCA) in a Ca^{2+}-free medium (0.1 mM EGTA added). This treatment resulted in a transient increase in $[Ca^{2+}]_i$ due to release of Ca^{2+} from ER followed by a rapid reduction in $[Ca^{2+}]_i$ (Fig. 3, trace a). It has been shown that 1 mM lanthanum effectively seals the cell to Ca^{2+} flow across the plasma membrane, blocking both Ca^{2+} entry and efflux [32]. While the TG-mediated increase in $[Ca^{2+}]_i$ was not influence by lanthanum treatment, the subsequent reduction in $[Ca^{2+}]_i$ was blocked (Fig. 3, trace b). This result demonstrates that the reduction in $[Ca^{2+}]_i$ observed in trace a was due to extrusion of calcium to the extracellular space.

The two main mechanisms of Ca^{2+} efflux across the plasma membrane are the Na^+/Ca^{2+} exchanger and PMCA [33]. Therefore, we inhibited the Na^+/Ca^{2+} exchanger by replacing the Na^+ in the growth media with 140 mM *N*-methyl-D-glycamine to determine its contribution to calcium efflux. This treatment had no effect on the transient increase and subsequent decrease in $[Ca^{2+}]_i$ observed after TG treatment, demonstrating that this pump was not involved in this process (Fig. 3, trace c).

We next tested the possible involvement of mitochondria in the removal of Ca^{2+} from cytosol. Cells were treated with 10 μg/ml

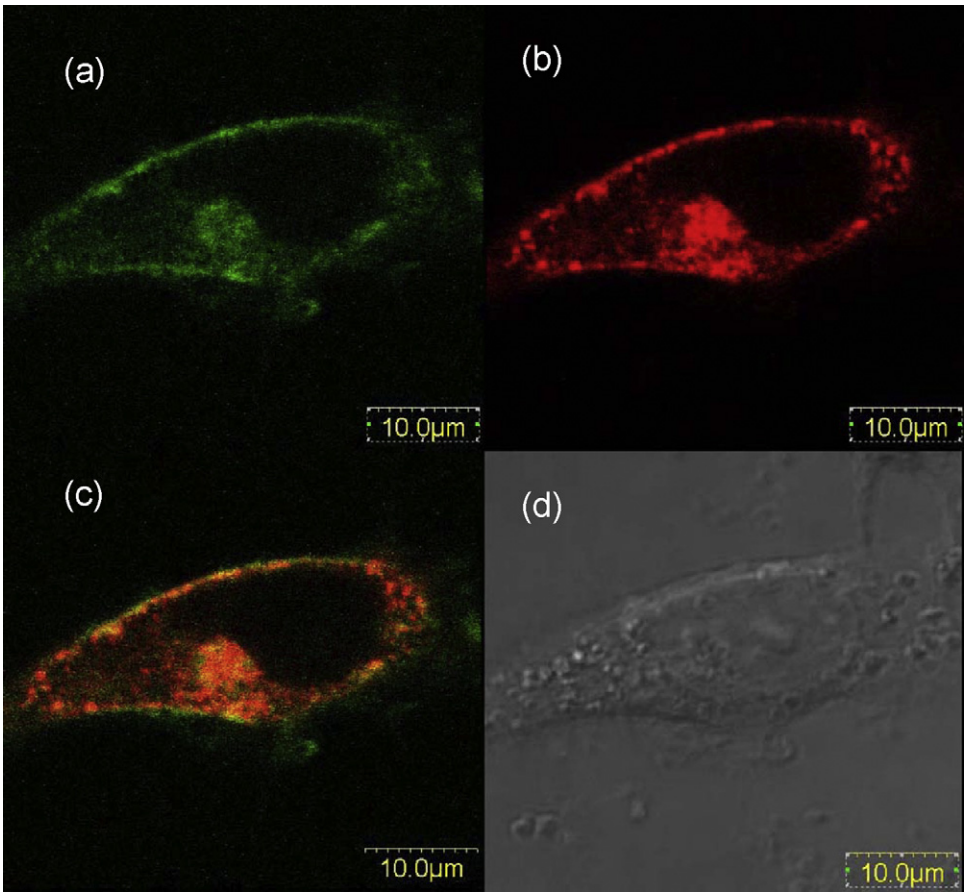

Fig. 2. Confocal imaging analysis of caveolin-1 and PMCA in ECV304 cells. EGFP–PMCA4b and ERFP–caveolin-1 plasmids were co-transfected into ECV304 cells. After 24 h of co-transfection, both PMCA–GFP (a), and caveolin-1-RFP (b) were supervised for their localizations. The superimposed image (c) showed the co-localization of PMCA and caveolin-1. Transmitted image of a transfected cell was also shown (d), bar = 10 μm.

oligomycin to inhibit F-ATPase, and thus eliminate Ca^{2+} uptake by mitochondria [34]. This treatment had no effect on the TG-mediated Ca^{2+} flux (data not shown). Collectively these data demonstrate that the Ca^{2+} efflux in our experimental conditions was mainly mediated by the PMCA.

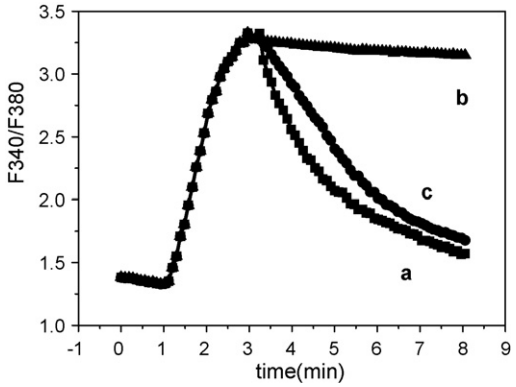

Fig. 3. PMCA was the major mechanism for the Ca^{2+} efflux in ECV304 cells. Fura-2-loaded ECV304 cells were stimulated with TG (5 μM) in a Ca^{2+}-free medium in the absence (a and c) or presence (b) of 1 mM $LaCl_3$. Elevations in $[Ca^{2+}]_i$ were monitored using the 340/380 fluorescence ratio. Trace (c) is in which Na^+ was completely replaced by *N*-methyl-D-glucamine (Na^+-free). Each trace represents the averages of about 120 cells in different chambers.

3.3. Inhibition of PMCA-mediated Ca^{2+} efflux by cholesterol depletion

As shown above, PMCA is localized to caveolae in ECV 304 cells and is redistributed after cholesterol depletion by MβCD. We wanted to determine the role of caveolar localization on PMCA function in the living cells. Therefore, we treated ECV 304 cells with 10 mM MβCD for 30 min and then measured the PMCA-mediated Ca^{2+} efflux following TG treatment. In control cells the rate of decay in Ca^{2+} concentration was $4.45 \pm 0.14\ min^{-1}$ (trace a). In contrast, MβCD treatment resulted in a reduction in this rate to $1.99 \pm 0.038\ min^{-1}$ (trace b), indicating that cholesterol depletion by MβCD significantly inhibited PMCA-mediated Ca^{2+} efflux. Importantly this reduction in Ca^{2+} efflux was not due to a loss of PMCA as the titer of this protein was the same in treated and control cells (data not shown). To confirm that the effects of MβCD on the PMCA-mediated Ca^{2+} efflux were due to removal of cholesterol, cholesterol-depleted ECV 304 cells were replenished by treatment with MβCD-cholesterol complex, which acts as a cholesterol donor. This treatment restored the rate of PMCA-mediated calcium decay to $3.79 \pm 0.19\ min^{-1}$ (Fig. 4, trace c).

3.4. Activity of PMCA reconstituted into liposomes

We wanted to determine if the lo phase state of caveolae was important for the activity of PMCA. Therefore we purified PMCA from erythrocytes and reconstituted the enzyme into lipo-

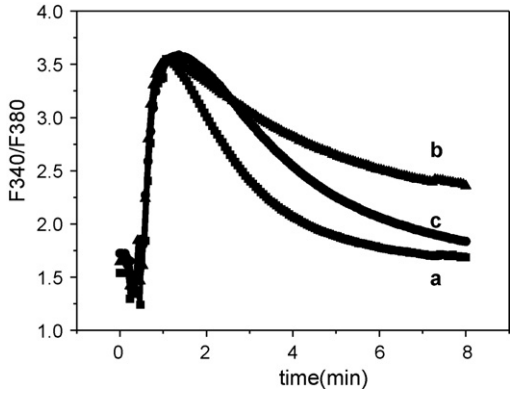

Fig. 4. Effect of MβCD on Ca^{2+} efflux in ECV 304 cells. Fura-2-loaded ECV304 cells were stimulated with TG (5 μM) in a Ca^{2+}-free medium without (trace a) and with (trace b) 10 mM MβCD treatment for 30 min. After treatment with 10 mM MβCD for 30 min, ECV304 cells were replenished with cholesterol (trace c). Each trace represents the averages of about 120 cells in different chambers.

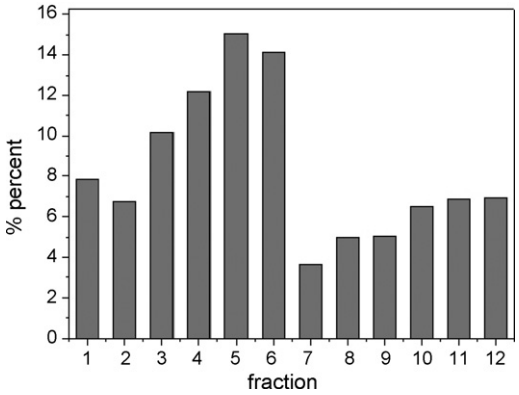

Fig. 6. Distribution of phophatidylserine in individual caveolae fractions. Caveolae of ECV304 cells were separated by sucrose density gradient centrifugation, total lipids of samples were extracted by chloroform/methanol and phosphatidylserine in each fraction was quantified by Annexin V-FITC.

somes composed of phosphatdylcholine (PC), sphingomyelin (SPM) and varying concentrations of cholesterol. As expected, membrane fluidity decreased with increasing cholesterol (Fig. 5a). Consistent with the previous reports [25], liposomes with a cholesterol concentration greater than 0.5 μmol were in the lo phase, similar to caveolae/lipid rafts. Unexpectedly, the ATPase activity of reconstituted PMCA decreased with increasing cholesterol concentrations (Fig. 5b), contradicting our observations in living cells. We reasoned that the simple lipid composition of our liposomes did not adequately model the complex lipid composition of the plasma membrane. Therefore, PMCA was reconstituted into liposomes prepared with lipids extracted from ECV 304 cells. The fluidity of liposomes prepared with plasma membrane lipids showed the cholesterol dependency (Fig. 5c). Furthermore, liposomes prepared from the cells treated with MβCD were more fluid than those prepared from cells that had cholesterol added back. Interestingly, the ATPase activity of the reconstituted PMCA tended to decease with cholesterol depletion. Importantly, the activity of the reconstituted PMCA was higher in the cholesterol-replenished liposomes (Fig. 5c). Similar results were found for the caveolar PMCA isolated from proximal kidney tubules [24]. These results suggest that the activity of

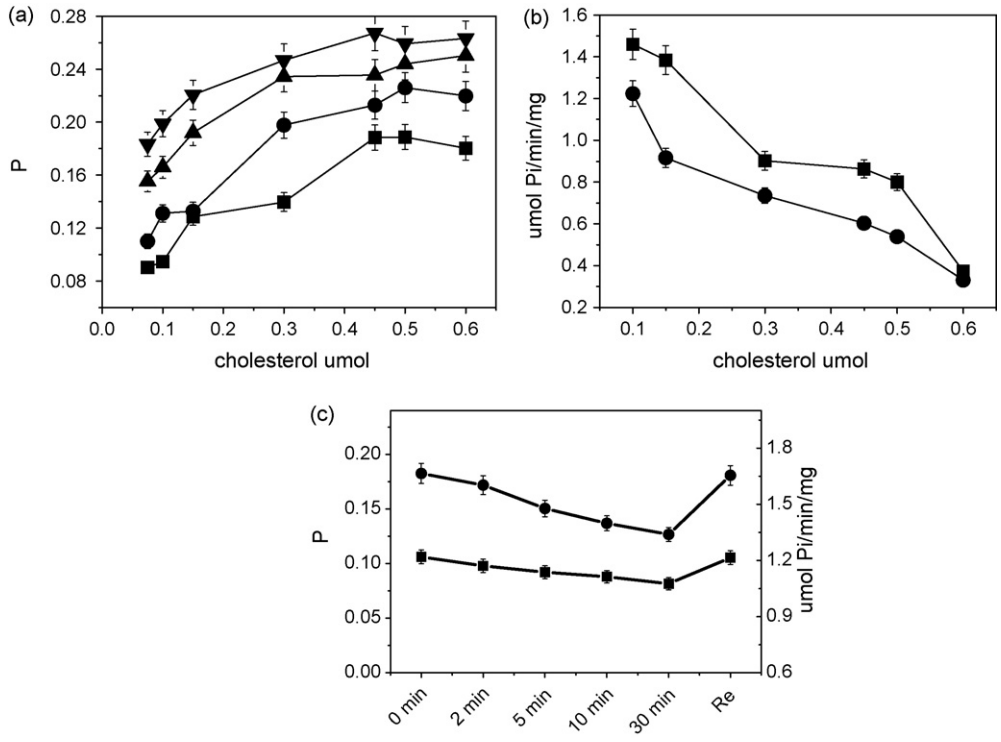

Fig. 5. Activities of PMCA reconstituted into sphingomyelin–cholesterol enriched liposomes. (a) The dependence of the fluorescence polarization (*P*) of DPH on cholesterol concentrations in liposomes containing cholesterol, PC and (■) 0 μmol; (●)0.05 μmol; (▲)0.15 μmol; (▼)0.25 μmol sphingomyelin. Total lipid was kept at 1 μmol. (b) The effect of cholesterol on the activity of PMCA reconstituted into liposomes containing (■) 0 μmol; (●) 0.25 μmol SPM, cholesterol and PC. Total lipid was kept at 1 μmol. (c) The fluorescence polarization (*P*) (●) of DPH and the activity of PMCA (■) reconstituted into liposomes resulted from lipids of ECV304 cells treated with MβCD for different time and cholesterol replenishments (Re). Data were expressed as mean ± S.D. from three-independent experiments.

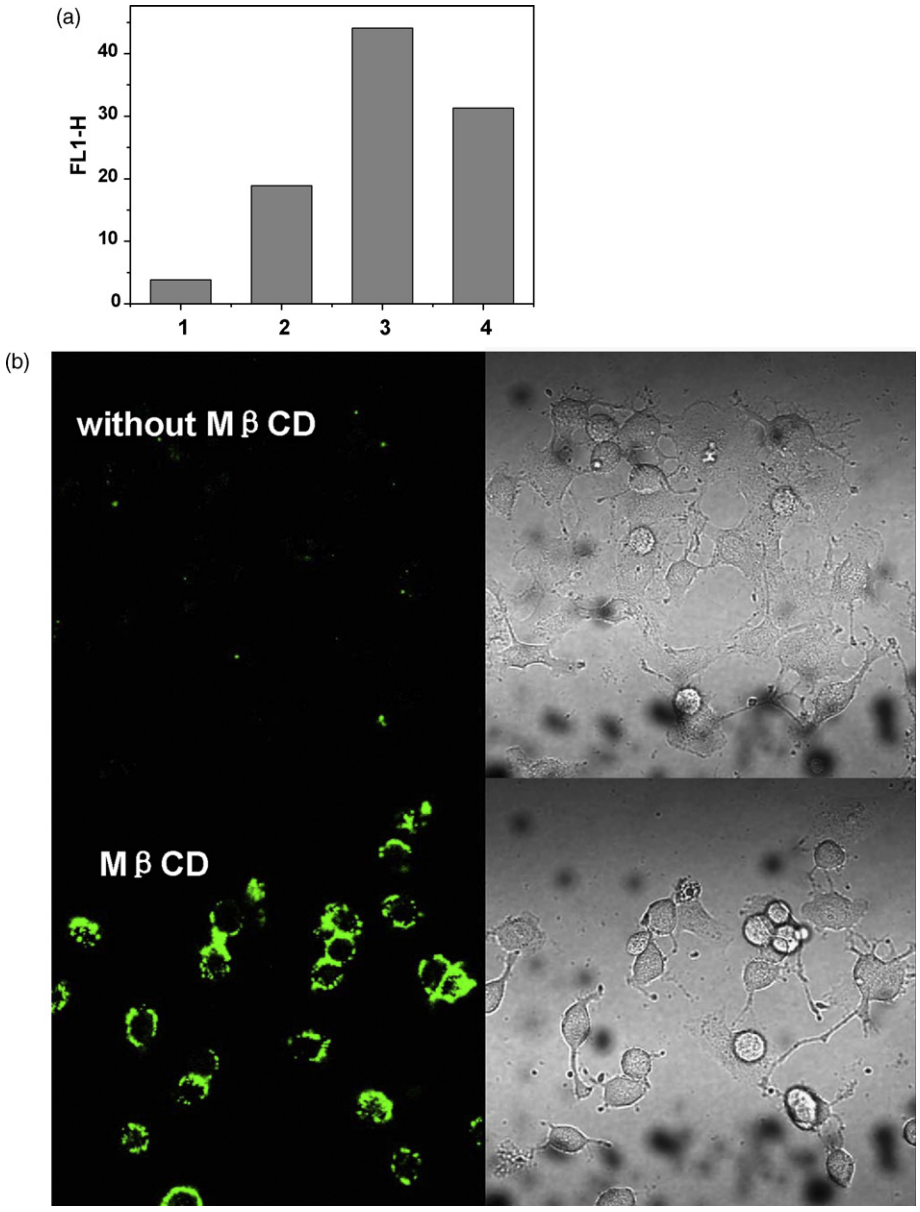

Fig. 7. MβCD treatment, lead to phosphatidylserine externalization in ECV304 cells. (a) PS externalization of the ECV304 was quantitatively determined by flow cytometry analysis. The cells were (1) unlabeled, (2) labeled with Annexin V-FITC probes, (3) labeled with probes and treated with MβCD and (4) labeled with probes and treated with MβCD then followed by cholesterol replenishment. Data were representative of three identical independent experiments. (b) PS probed by Annexin V-FITC was visualized by confocal microscopy. ECV304 cells labeled with Annexin V-FITC without (upper) and with (bottom) 10 mM MβCD treatment.

PMCA is dependent on specific lipids found in ECV 304 cell membranes.

3.5. Phosphatidylserine externalization by cholesterol depletion

It is known that PS is able to activate PMCA via direct interaction with the enzyme. To test the possible involvement of PS in the regulation of PMCA in living cells, we observed the movement of PS in respond to MβCD treatment. We first examined the PS distribution on the plasma membranes. As seen in Fig. 6, PS is found along the entire sucrose gradient, but is slightly enriched in the caveolae regions (fraction 3–6). It is known that PS is mostly sequestered in the inner leaflet of the plasma membrane. PS externalization was measured by flow cytometry using Annexin V-FITC, a widely used probe for PS [35–37]. The PS exposure on the surface of the plasma membranes was significantly increased after treatment with MβCD (Fig. 7a). In addition, the exposed PS was inwardly translocated when cholesterol depleted cells were replenished with cholesterol (Fig. 7a). The cholesterol-dependent externalization of PS was also detected using by confocal microscopy (Fig. 7b).

4. Discussion

Consistent with the reports about the localization of PMCA in caveolae/lipid rafts from cells and tissues, in the present study we also observed that PMCA is localized in caveolae from human umbilical vein endothelial ECV 304 cells. Importantly we have found that PMCA in caveolae from living cells is fully active, and this PMCA-mediated Ca^{2+} efflux is impaired by cholesterol depletion using MβCD. In addition, PS was exposed on the surface of the plasma membrane in the presence of MβCD, implying that the

PMCA-mediated Ca^{2+} efflux could be regulated by PS externalization in caveolae.

PMCA has been observed to localize in caveolae [22,23] or non-caveolar lipid rafts [38,39] from many cell types. However, little is known about how the caveolae/lipid raft environment influence the function of this enzyme. Although it has been reported that PMCA is active in isolated caveolae/lipid rafts [24,38], PMCA activity has not been investigated in the caveolae of living cells. Using our experimental conditions we were able to measure the activity of caveolae-localized PMCA in living cells. Because PMCA in ECV 304 cells is exclusively localized in caveolae as demonstrated by sucrose gradient fractionation, the observed PMCA-mediated Ca^{2+} efflux shown in Fig. 3 (trace a) reflects the PMCA functions in caveolae. To further demonstrate that the Ca^{2+} efflux resulted from caveolar PMCA, the cells were subjected to cholesterol depletion using MβCD. This compound is a well-known caveolae disruptor, which acts by sequestering cholesterol. We found that the PMCA-mediated Ca^{2+} efflux was significantly reduced in response to this treatment. In addition, the impaired Ca^{2+} efflux was almost completely restored after cholesterol replenishment. These results demonstrate for the first time that caveolae-localized PMCA is active and able to pump Ca^{2+} out of the cytosol in living cells.

The impaired Ca^{2+} efflux after MβCD treatment suggests that caveolae integrity is important for PMCA function. However, little is known about the mechanism by which PMCA activity is influenced by caveolae. To this end, we reconstituted purified PMCA into liposomes containing PC, SPM and cholesterol to simulate caveolae/lipid rafts in vitro. Surprisingly, the reconstituted PMCA showed reduced ATPase activity with increasing sphingomyelin-cholesterol ratio. As in our and other studies [25], the lipid mixture is mainly in lo phase, as are lipid rafts, if $\chi_{SPM-chol}$ is beyond 0.7 (cholesterol concentration is 0.5 μmol in our experiments shown in Fig. 5a). Therefore, our in vitro study suggests that PMCA in caveolae has lower activity than it would outside of these microdomains, which is consistent with other reports [25]. However, this result seems to contradict our observations in living cells. Negligible PMCA was found in non-caveolae plasma membranes of ECV 304, thus preventing a direct comparison of PMCA activity in and out of caveolae in vivo.

Interestingly, the activity of PMCA reconstituted into liposomes prepared with lipids extracted from cell membranes is positively correlated with cholesterol concentrations, which is consistent with our in vivo results and with a previous study of PMCA isolated from proximal kidney tubules [24]. Apparently, membrane fluidity alone cannot explain the activity of PMCA in the plasma membrane both in vitro and in vivo. These results in vitro indicate that specific lipids in the plasma membrane are required for maximal PMCA activity. However, it should be noted that PMCA4b isolated from cerebellum synaptic plasma membranes was shown to be localized in lipid rafts, but to have lower activity [38]. It is likely that the lipid compositions of cerebellum synaptic plasma membranes and ECV 304 are different. For example, cerebellum synaptic plasma membranes contain much more complicated gangliosides, which have been shown to regulate PMCA [40].

It is known that acidic phospholipids, including PS, are able to stimulate PMCA by direct interaction with the enzyme. Although sphingolipids and cholesterol, have been demonstrated to be enriched in caveolae/lipid rafts, some acidic lipids, such as PS, PI and PIP2 are also believed to be preferentially located in caveolae/lipid rafts [8]. We also found PS to be slightly enriched in caveolae from ECV 304 cells. PS is mostly sequestered in the inner leaflet of the plasma membrane, which we confirmed by flow cytometry using Annexin V-FITC. However, upon treatment with MβCD PS was externalized. The mechanism by which PS is externalized in the presence of MβCD is unknown, but cholesterol depletion clearly affects PS flip-flop. The movement of PS to the extracellular leaflet of the plasma membrane probably results in the dissociation of PS from PMCA, resulting in a reduction in activity.

It has been reported that PMCA is concentrated 18- to 25-fold in caveolae compared with the non-caveolae portion of the plasma membrane [22,23]. How this preferential localization is achieved is not yet known. A caveolin-binding motif containing the specific spacing (ϕXϕXXXXϕ, ϕXXXXϕXXϕ, or ϕXϕXXXXϕXXϕ, where ϕ=Trp, Phe, or Tyr) was proposed [41]. However, PMCA has no similar motif. In addition, caveolin and PMCA were found to not interact by immunoprecipitation (data not shown). We have demonstrated that PMCA4b is the predominant isoform in ECV 304 (Fig. 1a). It has been shown that a Cys residue near the C-terminus or in the loop between M2 and M3 could be palmitoylated, a modification that is essential for lipid rafts localization of PMCA4 in cerebellum synaptic plasma membranes [38]. Palmitoylation has also been demonstrated to be essential for the caveolae/lipid raft localization of other transmembrane proteins [42–44]. However, the role of palmitoylation in the caveolar localization of PMCA from ECV 304 is unknown.

It has been argued that PMCA is initially localized in caveolae where PMCA is inactive without Ca^{2+} stimulation [25]. In response to Ca^{2+}, PMCA could move out of caveolae and become fully active. This is unlikely since Ca^{2+} efflux after treatment with MβCD (PMCA is distributed in both in caveolae and non-caveolae domains) is reduced in comparison with that in the absence of MβCD (PMCA is predominantly in caveolae). In conclusion, the activity of PMCA in vitro is decreased with a decrease in membrane fluidity, suggesting that the environment in caveolae/rafts inhibits PMCA. On the other hand, the activation of PMCA in living cells indicates that the specific lipids such as PS in caveolae can stimulate PMCA. Therefore, both the physical state, such as membrane fluidity, and specific lipids, such as PS, of caveolae/lipid rafts contribute to the regulation of PMCA.

Acknowledgements

We thank Dr. John K. Zehmer (Cell Biology Department, UT Southwestern Medical Center) for his kind review of the manuscript. This work was supported by National Basic Research Program of China (2004CB720000 and 2006CB911001), and National Natural Science Foundation of China (30770492).

References

[1] R.G. Parton, K. Simons, The multiple faces of caveolae, Nat. Rev. Mol. Cell Biol. 8 (2007) 185–194.
[2] R.G. Anderson, The caveolae membrane system, Annu. Rev. Biochem. 67 (1998) 199–225.
[3] G.E. Palade, Fine structure of blood capillaries, J. Appl. Phys. 24 (1953) 14–24.
[4] E. Yamada, The fine structures of the gall bladder epithelium of the mouse, J. Cell Biol. 1 (1955) 445–458.
[5] U. Ortegren, M. Karlsson, N. Blazic, M. Blomqvist, F.H. Nystrom, J. Gustavsson, P. Fredman, P. Stralfors, Lipids and glycosphingolipids in caveolae and surrounding plasma membrane of primary rat adipocytes, Eur. J. Biochem. 271 (2004) 2028–2036.
[6] D.A. Brown, J.K. Rose, Sorting of GPI-anchored proteins to glycolipid-enriched membrane subdomains during transport to the apical cell surface, Cell 68 (1992) 533–544.
[7] K. Fiedler, T. Kobayashi, T.V. Kurzchalia, K. Simons, Glycosphingolipid-enriched, detergent-insoluble complexes in protein sorting in epithelial cells, Biochemistry 32 (1993) 6365–6373.
[8] L.J. Pike, X. Han, K.N. Chung, R.W. Gross, Lipid rafts are enriched in arachidonic acid and plasmenylethanolamine and their composition is independent of caveolin-1 expression: a quantitative electrospray ionization/mass spectrometric analysis, Biochemistry 41 (2002) 2075–2088.
[9] P.F. Devaux, Static and dynamic lipid asymmetry in cell membranes, Biochemistry 30 (1991) 1163–1173.
[10] S. Uhles, T. Moede, B. Leibiger, P.O. Berggren, I.B. Leibiger, Isoform-specific insulin receptor signaling involves different plasma membrane domains, J. Cell Biol. 163 (2003) 1327–1337.

[11] M. Kai, F. Sakane, Y.J. Jia, S. Imai, S. Yasuda, H. Kanoh, Lipid phosphate phosphatases 1 and 3 are localized in distinct lipid rafts, J. Biochem. (Tokyo) 140 (2006) 677–686.
[12] M. St Maurice, L. Reinhardt, K.H. Surinya, P.V. Attwood, J.C. Wallace, W.W. Cleland, I. Rayment, Domain architecture of pyruvate carboxylase, a biotin-dependent multifunctional enzyme, Science 317 (2007) 1076–1079.
[13] E. Carafoli, Calcium pump of the plasma membrane, Physiol. Rev. 71 (1991) 129–153.
[14] F. Wuytack, L. Raeymaekers, The Ca^{2+}-transport ATPases from the plasma membrane, J. Bioenerg. Biomembr. 24 (1992) 285–300.
[15] E. Carafoli, Biogenesis: plasma membrane calcium ATPase: 15 years of work on the purified enzyme, FASEB J. 8 (1994) 993–1002.
[16] R.M. Gopinath, F.F. Vincenzi, Phosphodiesterase protein activator mimics red blood cell cytoplasmic activator of (Ca^{2+}–Mg^{2+}) ATPase, Biochem. Biophys. Res. Commun. 77 (1977) 1203–1209.
[17] H.W. Jarrett, J.T. Penniston, Partial purification of the Ca^{2+}–Mg^{2+} ATPase activator from human erythrocytes: its similarity to the activator of 3′,5′-cyclic nucleotide phosphodiesterase, Biochem. Biophys. Res. Commun. 77 (1977) 1210–1216.
[18] V. Niggli, E.S. Adunyah, E. Carafoli, Acidic phospholipids, unsaturated fatty acids, and limited proteolysis mimic the effect of calmodulin on the purified erythrocyte Ca^{2+}-ATPase, J. Biol. Chem. 256 (1981) 8588–8592.
[19] P. Brodin, R. Falchetto, T. Vorherr, E. Carafoli, Identification of two domains which mediate the binding of activating phospholipids to the plasma-membrane Ca^{2+} pump, Eur. J. Biochem. 204 (1992) 939–946.
[20] A.G. Filoteo, A. Enyedi, J.T. Penniston, The lipid-binding peptide from the plasma membrane Ca^{2+} pump binds calmodulin, and the primary calmodulin-binding domain interacts with lipid, J. Biol. Chem. 267 (1992) 11800–11805.
[21] E. Zvaritch, P. James, T. Vorherr, R. Falchetto, N. Modyanov, E. Carafoli, Mapping of functional domains in the plasma membrane Ca^{2+} pump using trypsin proteolysis, Biochemistry 29 (1990) 8070–8076.
[22] T. Fujimoto, Calcium pump of the plasma membrane is localized in caveolae, J. Cell Biol. 120 (1993) 1147–1157.
[23] J.E. Schnitzer, P. Oh, B.S. Jacobson, A.M. Dvorak, Caveolae from luminal plasmalemma of rat lung endothelium: microdomains enriched in caveolin, Ca^{2+}-ATPase, and inositol trisphosphate receptor, Proc. Natl. Acad. Sci. 92 (1995) 1759–1763.
[24] G.G. Tortelote, R.H. Valverde, T. Lemos, A. Guilherme, M. Einicker-Lamas, A. Vieyra, The plasma membrane Ca^{2+} pump from proximal kidney tubules is exclusively localized and active in caveolae, FEBS Lett. 576 (2004) 31–35.
[25] Y. Pang, H. Zhu, P. Wu, J. Chen, The characterization of plasma membrane Ca^{2+}-ATPase in rich sphingomyelin-cholesterol domains, FEBS Lett. 579 (2005) 2397–2403.
[26] H. Haaker, E. Racker, Purification and reconstitution of the Ca^{2+}-ATPase from plasma membrane of pig erythrocytes, J. Biol. Chem. 254 (1979) 6598–6602.
[27] D. Gingras, F. Gauthier, S. Lamy, R.R. Desrosiers, R. Beliveau, Localization of RhoA GTPase to endothelial caveolae-enriched membrane domains, Biochem. Biophys. Res. Commun. 247 (1998) 888–893.
[28] M. Shinitzky, Y. Barenholz, Fluidity parameters of lipid regions determined by fluorescence polarization, Biochim. Biophys. Acta 515 (1978) 367–394.
[29] P.Y. Wang, J.W. Chen, F. Hwang, Anisodamine causes acyl chain interdigitation in phosphatidylglycerol, FEBS Lett. 332 (1993) 193–196.
[30] Y.M. Usachev, S.J. DeMarco, C. Campbell, E.E. Strehler, S.A. Thayer, Bradykinin and ATP accelerate Ca^{2+} efflux from rat sensory neurons via protein kinase C and the plasma membrane Ca^{2+} pump isoform 4, Neuron 33 (2002) 113–122.
[31] J.A. Rosado, S.O. Sage, Regulation of plasma membrane Ca^{2+}-ATPase by small GTPases and phosphoinositides in human platelets, J. Biol. Chem. 275 (2000) 19529–19535.
[32] E.C. Toescu, O.H. Petersen, Pflu. Arch. 444 (1994) 325–331.
[33] T.J. Rink, S.O. Sage, Stimulated calcium efflux from fura-2-loaded human platelets, J. Physiol. 393 (1987) 513–524.
[34] C.Y. Kwan, H. Takemura, J.F. Obie, O. Thastrup, J.W. Putney Jr., Effects of MeCh, thapsigargin, and La^{3+} on plasmalemmal and intracellular Ca^{2+} transport in lacrimal acinar cells, Am. J. Physiol. 258 (1990) C1006–C1015.
[35] C. Kunzelmann-Marche, J.M. Freyssinet, M.C. Martinez, Loss of plasma membrane phospholipid asymmetry requires raft integrity. Role of transient receptor potential channels and ERK pathway, J. Biol. Chem. 277 (2002) 19876–19881.
[36] K. Fischer, S. Voelkl, J. Berger, R. Andreesen, T. Pomorski, A. Mackensen, Antigen recognition induces phosphatidylserine exposure on the cell surface of human CD8+T cells, Blood 108 (2006) 4094–4101.
[37] X. Wang, J. Wang, K. Gengyo-Ando, L. Gu, C.L. Sun, C. Yang, Y. Shi, T. Kobayashi, Y. Shi, S. Mitani, X.S. Xie, D. Xue, *C. elegans* mitochondrial factor WAH-1 promotes phosphatidylserine externalization in apoptotic cells through phospholipid scramblase SCRM-1, Nat. Cell Biol. 9 (2007) 541–549.
[38] M.R. Sepulveda, M. Berrocal-Carrillo, M. Gasset, A.M. Mata, The plasma membrane Ca^{2+}-ATPase isoform 4 is localized in lipid rafts of cerebellum synaptic plasma membranes, J. Biol. Chem. 281 (2006) 447–453.
[39] L. Jiang, D. Fernandes, N. Mehta, J.L. Bean, M.L. Michaelis, A. Zaidi, Partitioning of the plasma membrane Ca^{2+}-ATPase into lipid rafts in primary neurons: effects of cholesterol depletion, J. Neurochem. 102 (2007) 378–388.
[40] J. Zhang, Y.F. Zhao, J.F. Duan, F.Y. Yang, X. Zhang, Gangliosides activate the phosphatase activity of the erythrocyte plasma membrane Ca^{2+}-ATPase, Arch. Biochem. Biophys. 44 (2005) 1–6.
[41] J. Couet, S. Li, T. Okamoto, T. Ikezu, M.P. Lisanti, Identification of peptide and protein ligands for the caveolin-scaffolding domain. Implications for the interaction of caveolin with caveolae-associated proteins, J. Biol. Chem. 272 (1997) 6525–6533.
[42] W. Zhang, R.P. Trible, L.E. Samelson, LAT palmitoylation: its essential role in membrane microdomain targeting and tyrosine phosphorylation during T cell activation, Immunity 9 (1998) 239–246.
[43] S. Arni, S.A. Keilbaugh, A.G. Ostermeyer, D.A. Brown, Association of GAP-43 with detergent-resistant membranes requires two palmitoylated cysteine residues, J. Biol. Chem. 273 (1998) 28478–28485.
[44] R. Fragoso, D. Ren, X. Zhang, M.W. Su, S.J. Burakoff, Y.J. Jin, Lipid raft distribution of CD4 depends on its palmitoylation and association with Lck, and evidence for CD4-induced lipid raft aggregation as an additional mechanism to enhance CD3 signaling, J. Immunol. 170 (2003) 913–921.